IOP Conf. Series: Journal of Physics: Conf. Series **878** (2017) 012015 doi:10.1088/1742-6596/878/1/012015

The Beam Energy Scan at the Relativistic Heavy Ion Collider

Declan Keane

Department of Physics, Kent State University, Kent, Ohio 44242, USA

E-mail: keane@kent.edu

Abstract. The Beam Energy Scan (BES) at the Relativistic Heavy Ion Collider (RHIC) is based on Au + Au collision data acquired between 2010 and 2014 at beam energies of $\sqrt{s_{NN}}$ = 7.7, 11.5, 14.5, 19.6, 27 and 39 GeV. These measurements constitute Phase-I of BES (also known as BES-I), and along with higher-energy data at 62.4 and 200 GeV, they allow the phase diagram of QCD matter to be probed. BES-I has three physics goals: investigation of a turning-off of the Quark-Gluon Plasma (QGP) signatures that are by now well established at higher energies, the search for a possible first-order phase transition between hadronic and QGP phases, and the search for a possible critical point. Several promising signals have been reported, but since RHIC luminosity decreases steeply as the beam energy is scanned down, statistical errors are excessively large at the lower BES-I energies where potentially novel phenomena are observed. In 2019 and 2020, BES-II will take data with large improvements in both RHIC luminosity and in detector performance.

1. Introduction

During the years 2000 to 2010, corresponding to the first decade of operation of the Relativistic Heavy-Ion Collider at Brookhaven National Laboratory, the physics focus was on gold-gold collisions at $\sqrt{s_{NN}}$ = 200 GeV [1, 2, 3, 4]. During that period, there was an accumulation of evidence pointing to the production of a deconfined partonic phase in the early stages of the collisions when the energy density is high. Our current understanding is illustrated by the conceptual phase diagram on the left in Fig. 1. Lattice QCD calculations [5, 6, 7] indicate that the transition is a smooth crossover at top RHIC energies and above. By colliding nuclei at progressively lower energies, it should be possible to probe phase diagram regions of increasingly high baryon chemical potential μ_B (equivalent to increasingly high density of baryons minus antibaryons), exploring the possible region of a first-order phase transition and the vicinity of the associated critical end point. Lattice calculations suggest that the critical point does not lie at or below $\mu_B \sim 250$ MeV [8, 9, 10, 11]. However, our knowledge to date from theory and experiment does not exclude the possibility that a crossover extends to much higher baryon chemical potentials than depicted on the left in Fig. 1.

The first physics goal of the BES-I program is to investigate the expected turning-off of the Quark-Gluon Plasma (QGP) signatures that are by now well established at higher collision energies. A disappearance of these signatures would not necessarily flag the location on the phase diagram where the deconfined phase begins, since factors unrelated to the onset of deconfinement might weaken or even completely obscure individual signatures as the beam energy is scanned down. For example, jet quenching may disappear at lower beam energies simply because all

hard scattering effects become rare at lower beam energies, as the high-p_T regions are much less populated. However, if it is observed that a few independent signatures all point to a turn-off at about the same beam energy, a more convincing inference might be reached.

The second BES-I goal is to search for the predicted first-order phase transition [12, 13] between hadronic and QGP phases. Observables like anisotropic flow are promising for this purpose, since flow is a proxy for the pressure in a hydrodynamic picture. As the beam energy increases above the region where the system is always in a hadronic phase, new degrees of freedom begin to open up, and spinodal decomposition and a long-lived mixed phase may play important roles. In some models, there can be a dramatic drop in the pressure, or using equivalent terminology, there is a softening of the Equation of State (EOS) at a bombarding energy where the system first reaches a region where there is a first-order phase transition [14, 15].

The third goal is to search for a possible critical end point, which must be present if the phase diagram includes a first-order phase transition. The characteristic length scale in a macroscopic system (the correlation length) becomes infinite at a critical point, and causes observable effects such as critical opalescence. In a small system such as in a heavy-ion collision, the potential for growth of the correlation length is very limited, but theory still suggests that the local increase in fluctuations caused by a critical point could be observed experimentally [16].

2. BES-I and freeze-out parameters

The STAR detector [17] is well suited for investigating the physics objectives outlined above. In contrast to fixed target experiments, STAR has the advantage that its acceptance changes relatively little as $\sqrt{s_{NN}}$ is scanned from 7.7 to 39 GeV. Furthermore, STAR offers a large and uniform acceptance in azimuthal angle and transverse momentum in the midrapidity region, with excellent particle identification through dE/dx and Time-of-Flight [18], allowing many observables and their correlations to be measured. These detector characteristics make optimum use of the very limited statistics available towards the low end of the BES-I range, where RHIC's luminosity drops very steeply.

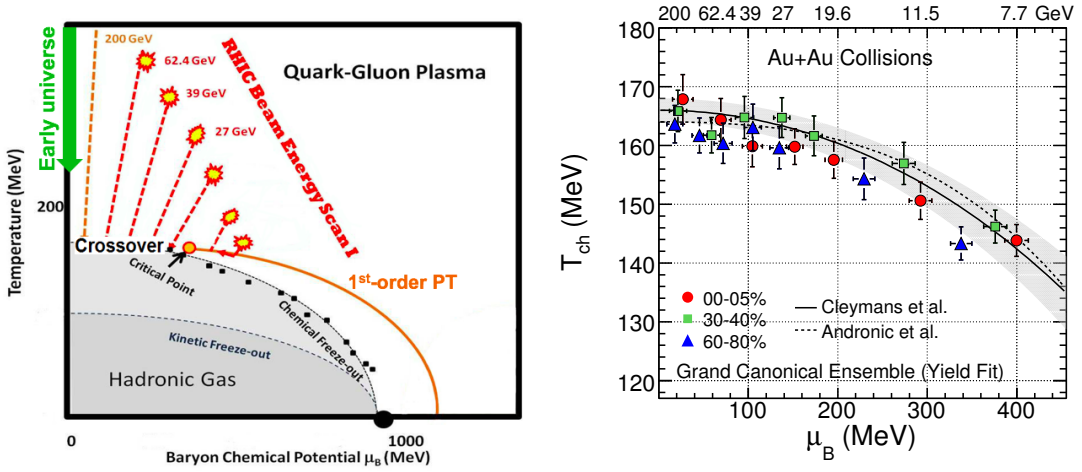

Figure 1. Left panel: A conceptual QCD phase diagram, showing the relevant regions in the plane of T versus μ_B. Various details, especially the position of the critical point, are highly uncertain. Right panel: Inferred coordinates of chemical freeze-out in the plane of T versus μ_B, for various beam energies (see upper horizontal scale) and centralities, based on measured particle spectra [19] and a thermal model [20].

In 2010, 2011 and 2014, the original RHIC measurements at $\sqrt{s_{NN}} = 200$ and 62.4 GeV were extended to lower beam energies in the form of the BES-I data at 39, 27, 19.6, 14.5, 11.5, and 7.7 GeV. These $\sqrt{s_{NN}}$ values correspond to baryon chemical potentials in the range 25 to about 400 MeV [19, 20] (see panel on the right of Fig. 1). This correspondence is determined by combining measured spectra for identified particles with a thermal model to infer the position on the phase diagram where interactions that can change the particle species cease (chemical freeze-out), and any subsequent interactions are elastic only. The panel on the right of Fig. 1 suggests that the existing set of BES-I measurements offers adequate coverage of the phase diagram near and below $\mu_B \sim 400$ MeV.

As of the end of 2016, STAR's BES-I effort has resulted in 18 published journal papers with final results [21, 22, 23, 24, 25], with several more in the pipeline. The final published BES papers account for about one-third of the total physics output from the STAR collaboration since 2012. There have also been many proceedings that cover recent preliminary results from BES-I. The present proceedings have space to touch on only a subset of BES-I findings and on the outlook for BES-II.

3. Directed flow of protons

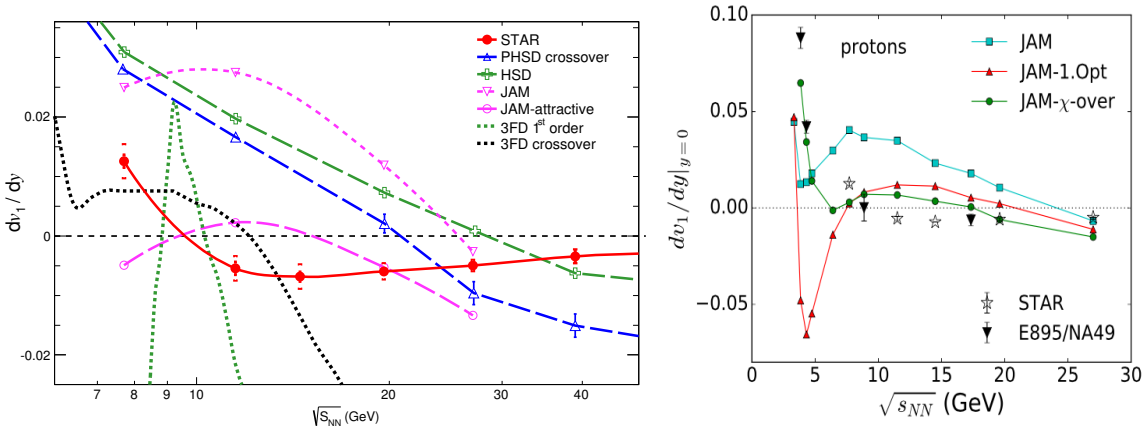

Figure 2. Left panel: Directed flow slope dv_1/dy near midrapidity as a function of beam energy for protons in 10-40% centrality Au+Au collisions from STAR [21], compared with recent models [26, 27, 28], as compiled in Ref. [29]. Other recent model comparisons [30] lie above the experimental data and are off-scale at all plotted beam energies. Right panel: A comparison between the same STAR dv_1/dy data and a new prescription for incorporating the EOS and the possible phase change in the JAM transport model [31]. The red triangle markers correspond to the EOS option with a first-order phase transition.

The first harmonic coefficient in the Fourier expansion of the distribution of azimuths ϕ of final-state particles relative to the event reaction plane azimuth $\Psi_{\rm RP}$, is known as directed flow: $v_1 = \langle \cos(\phi - \Psi_{\rm RP}) \rangle$ [32, 33, 34]. It describes a collective sideward deflection of the emitted particles. Models in the nuclear transport [35, 36] and hydrodynamic [37] categories support the interpretation that directed flow is a good probe of the participant matter during the early stages of the collision [38, 39, 40], e.g., can serve as a signature of the pressure. The slope of the rapidity dependence dv_1/dy close to mid-rapidity is a convenient way to characterize the overall magnitude of the directed flow signal. In particular, STAR's measurements at $\sqrt{s_{NN}} = 7.7$ to 200 GeV reveal that proton directed flow goes through a minimum between 10 and 20 GeV [21, 41]. Three-fluid hydrodynamic calculations [14, 15] qualitatively predicted this minimum,

dubbed the "softest point collapse", and reported this model behavior when the EOS has a first-order phase transition, but not when the EOS is hadronic only.

Following the publication of the first set of STAR BES results for directed flow [21], several theorists reported model comparisons incorporating various options for the assumed EOS [26, 27, 28, 30, 31]. Generally, these theorists conclude that an assumption of purely hadronic physics is not favored, whereas they are divided on the issue of whether a crossover or first-order phase transition is closer to the STAR measurements. No EOS option in any of these models gives rise to a minimum in proton directed flow anywhere close in beam energy to the measured minimum [26, 27, 28, 30, 42] with the arguable exception of Nara *et al.* [31], whose most recent paper, in the case of a first-order phase transition, reports a minimum that is about an order of magnitude deeper than the measured one, and lies about a factor of three lower in beam energy (see Fig. 2). Furthermore, for equations of state that are nominally the same (e.g., either crossover or first order), directed flow from different model implementations are often very widely divergent, at the level of an order of magnitude larger than the measured signal and two orders larger than the measured errors [29]. Therefore, in order to reach a definite conclusion about the nature of the transition, further progress in the area of model calculations of $v_1(y)$ is needed. This is an active area for the BEST topical theory collaboration. On the experimental side, new directed flow measurements for more baryon species, and in fine centrality bins, will further constrain models and will help resolve the pending questions [21, 41, 43].

4. The Chiral Magnetic Effect

The non-trivial structure of the QCD vacuum is a topic of high importance, and many open questions remain. There is a family of quantum phenomena that can arise from interactions with the very high vorticity and the exceptionally intense localized magnetic field ($\sim 10^{15}$ T) that are briefly generated during non-central collisions of heavy ions. Differences in the number of left-handed and right-handed quarks in the QGP can cause a characteristic signature of charge separation along the magnetic field. These considerations are not just relevant to relativistic heavy ion physics, but have implications for all areas of physics touched by QCD (high energy physics, astrophysics, cosmology, etc.) A number of related anomalous chiral effects are discussed in the literature, but the primary one is known as the Chiral Magnetic Effect (CME). Many articles examine these topics in depth [44, 45, 46, 47, 48, 49, 50, 51] and the interested reader should consult the extensive reference list in the recent review by Kharzeev *et al.* [51].

For the purpose of the present brief summary of BES-I physics, we set aside the broad implications outlined above, and simply note that a deconfined state (QGP) is needed to generate a true CME signal. Then we focus purely on the potential for our CME observable (the three-point correlator defined below) to flag the beam energy where QGP turns-off as we scan down in beam energy.

In a description of azimuthally anisotropic emission, $(dN_{\pm}/d\phi) \propto 1 + 2a_{\pm}\sin(\phi - \Psi_{\rm RP}) + ...$ the coefficient a represents the size of the CME signal, and the remaining terms (not shown explicitly) are the familiar cosines weighted by coefficients v_n for directed flow, elliptic flow, triangular flow, etc. The coefficient a averages to zero when integrated over many events. If chiral magnetism is present, a non-zero average signal can be obtained by forming a correlation between pairs of emitted particles relative to the reaction plane, in the form of the three-point correlator γ as defined in the expression along the vertical axis in Fig. 3, where α and β denote the particle type: α, $\beta = +, -$. In that case, the CME signature is the non-zero difference between $\gamma_{\rm SS}$ (same charge, plotted as red stars) and $\gamma_{\rm OS}$ (opposite charge, plotted as blue circles) in Fig. 3.

As expected in the presence of CME, we indeed see a signal in the form of a significant positive $\gamma_{\rm OS} - \gamma_{\rm SS}$ which grows steadily as we move from central to peripheral collisions, except at the two lowest beam energies, where $\gamma_{\rm OS} - \gamma_{\rm SS}$ is consistent with zero at all centralities. One

interpretation is that QGP is no longer produced at those lower energies.

Background effects, unrelated to CME, are argued to have a different centrality dependence and a different energy dependence to that shown by $\gamma_{\rm OS}$ and $\gamma_{\rm SS}$. However, specific theoretical calculations of the γ correlators are very challenging, and so far are lacking, and elliptic flow and conservation effects cannot be decisively ruled out as the origin of the signal $\gamma_{\rm OS} - \gamma_{\rm SS}$.

A future isobar measurement [53] in which collisions of $^{96}_{40}$Zr + $^{96}_{40}$Zr and $^{96}_{44}$Ru + $^{96}_{44}$Ru will be directly compared offers a robust and unambiguous way to settle this issue of possible elliptic-flow-related background effects in $\gamma_{\rm OS} - \gamma_{\rm SS}$. This measurement ought to be decisive, because the background scales with the total mass number of the initial system, which is the same for both pairs of incoming nuclei, while the true CME signal scales with the total electric charge of the initial system, which differs by 10% between Zr + Zr and Ru + Ru. This isobar measurement is scheduled to take data in 2018.

5. Search for the QCD critical point via net-proton fluctuations

Local fluctuations of conserved numbers like net electric charge or net baryon number increase near a critical point, and are considered to be among the most promising signatures. While such quantities cannot fluctuate globally (for an entire event), STAR measurements fall well short of being global, especially in regard to rapidity acceptance [54]. High moments like skewness, $S \propto \langle (N - \langle N \rangle)^3 \rangle$ and kurtosis, $\kappa \propto \langle (N - \langle N \rangle)^4 \rangle$ are of particular interest. Kurtosis is proportional to the seventh power of the correlation length, and notwithstanding the trivial increase of statistical errors with higher powers, it has been shown that high moments such as κ offer the best sensitivity to the fluctuations of interest [55, 56, 57, 16]. Another advantage of kurtosis and similar quantities is the fact that they can readily be calculated by lattice QCD [58].

High moments of net charge have been reported by both PHENIX [59] and STAR [23] at BES-I energies, but only monotonic behavior is observed. Experimental measurement of net baryons is very difficult, and net protons serve as a useful alternative observable. However, complicating factors such as resonance decays, hadronic scattering, etc., need to be taken into consideration when using net protons as a proxy for net baryons [60].

In Fig. 4 [61], it is evident that at centralities of 30-40% and 70-80%, $\kappa\sigma^2$ for net protons is

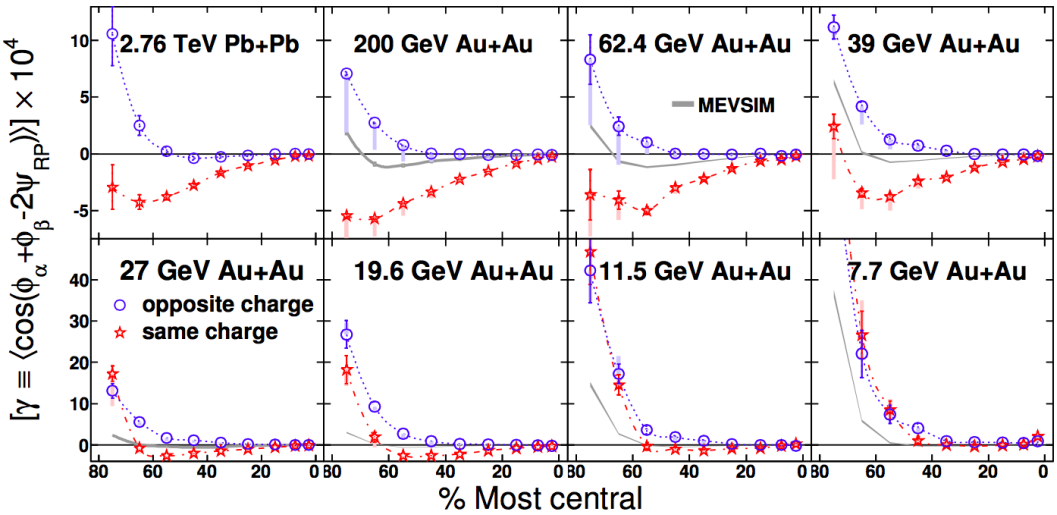

Figure 3. The three-point correlator γ as a function of centrality for Au+Au collisions from 200 GeV to 7.7 GeV [22]. ALICE results for Pb+Pb collisions at 2.76 TeV are also shown [52].

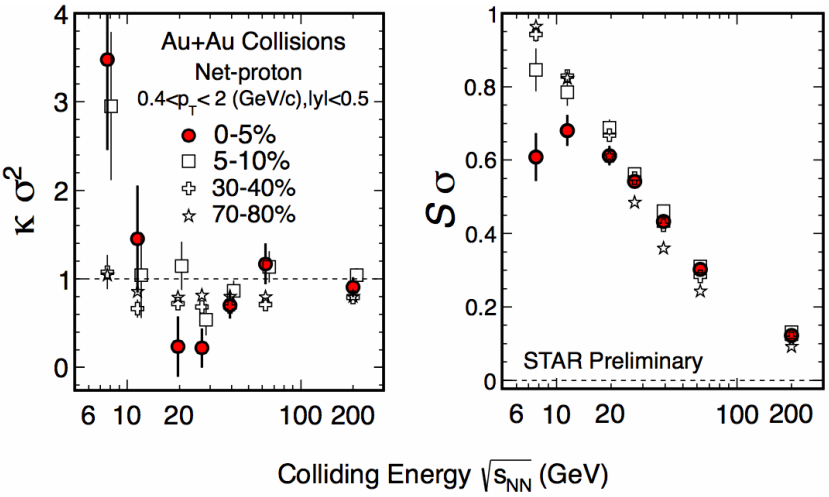

Figure 4. The dimensionless products $\kappa\sigma^2$ and $S\sigma$ for net protons as a function of beam energy in four centrality intervals [61]. The acceptance window for counting protons and antiprotons is $0.4 < p_T < 2.0$ GeV/c, $|y| < 0.5$. The kurtosis point for 0-5% centrality at 7.7 GeV is highly sensitive to efficiency corrections.

close to the baseline of 1.0 across all beam energies. However, for the red points (0-5% centrality), there is a minimum of moderate significance below the baseline centered near 20 GeV, with a steep rise as the beam energy is scanned further down, ending with a value about 2 standard errors above the baseline at 7.7 GeV. If this is a critical point signature of the kind predicted by Stephanov [16], $\kappa\sigma^2$ ought to return to the baseline value of unity at energies below 7.7 GeV. This observation strongly motivates exploration of beam energies below 7.7 GeV in the second phase of the beam energy scan (see Section 8 below).

6. Search for the QCD critical point via pion interferometry

Femtoscopy correlations [62] continue to evolve right up until kinetic freeze-out at the very end of the collision process. Nevertheless, this does not exclude the possibility that pion interferometry measurements provide sensitivity to EOS effects from a much earlier stage of the time evolution. Models suggest that such a sensitivity is present at a useful level [62].

The parameters $R_{\rm out}$, $R_{\rm side}$ and $R_{\rm long}$ are commonly used to orthogonally decompose the Gaussian radii for the spatial homogeneity regions from interferometry, and the difference $R^2_{\rm out} - R^2_{\rm side}$ is related to the time duration of emission [62]. Fig. 5 presents Lacey's compilation [63] of pion interferometry parameters $R^2_{\rm out} - R^2_{\rm side}$ in seven centrality intervals for Au + Au collisions at beam energies of 7.7, 11.5, 19.6, 27, 39, 62.4, and 200 GeV [24] and also for Pb + Pb collisions at 2.76 TeV [64]. From the observed peaks in $R^2_{\rm out} - R^2_{\rm side}$, one can infer a lengthening of the duration of pion emission, with the maxima occurring in the range of $\sqrt{s_{NN}} = 20$ to 40 GeV along the beam energy axis. It is also noteworthy that the beam energy of the peak drops smoothly as the collisions become less central. The peak also becomes smaller and its width increases as the collisions become less central.

Lacey [63] has interpreted these data under the assumption of Finite Size Scaling (FSS) behavior and critical exponents in the context of a 3D Ising model universality class [65, 66, 67]. In Ref. [63], it is argued that the data at all seven centralities vary according to the expected FSS behavior, as illustrated by all the points accurately mapping onto a common curve [63]. A chance occurrence of this scaling behavior would be highly improbable. This leads to the inference that the favored location of the critical point in this analysis is $(T,\, \mu_B)_{\rm crit} \sim (165,\, 95)$

MeV. This surprisingly low baryon chemical potential of 95 MeV at the inferred critical point does not appear to be compatible with lattice calculations, which rule out values below about 250 MeV [8, 9, 10, 11].

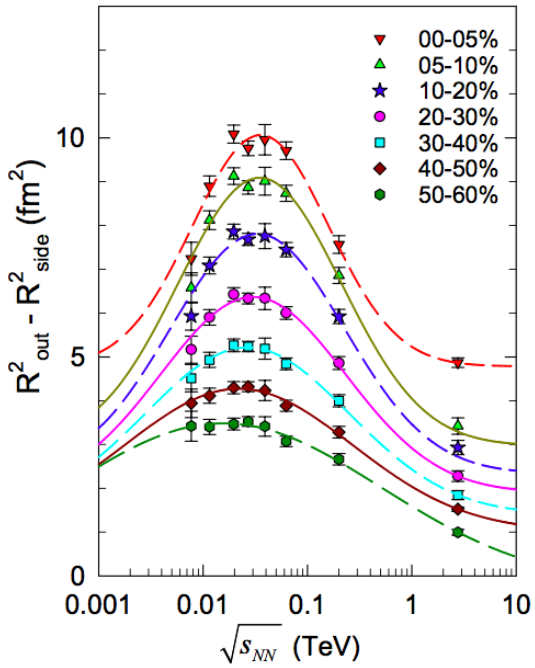

Figure 5. Pion femtoscopy parameters $R^2_{\rm out} - R^2_{\rm side}$ versus beam energy, covering Au + Au collisions at RHIC BES-I energies [24] through Pb + Pb at 2.76 TeV [64], in seven centrality intervals.

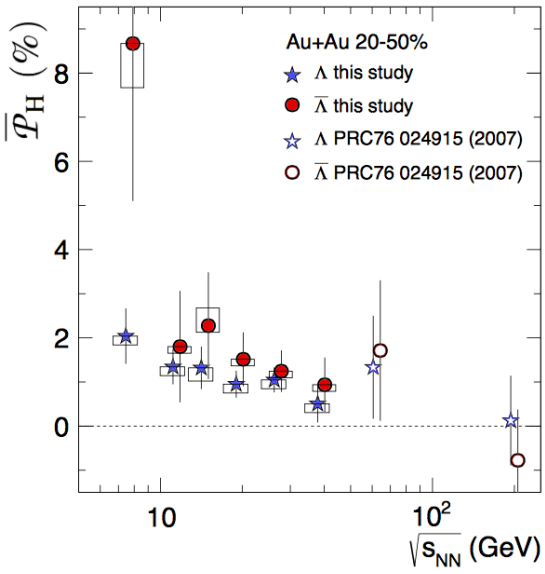

Figure 6. Average global polarization for Λ (stars) and anti-Λ (circles) produced in Au + Au collisions at 20-50% centrality as a function of beam energy. Results at 62.4 and 200 GeV, published by the STAR collaboration in 2007 [68], are presented along with recent measurements at BES-I energies [69]. Systematic errors are indicated by boxes.

7. Vorticity inferred from global polarization of Λ and anti-Λ

The Λ decay has the well-known 'self-analyzing' property whereby the daughter proton is preferentially emitted along the spin direction of the parent [70]. In *pp* collisions, this directly results in an observed Λ polarization at forward angles [71]. However, a 2007 search for the quite different phenomenon of global polarization in heavy-ion collisions at top RHIC energies yielded a null signal [68]. The term 'global' refers to an average over all (anti-)Λ momenta projected onto the angular momentum vector of each event before averaging over the available events. The reaction plane azimuth $\Psi_{\rm RP}$ is the basis for determining the direction of each event's angular momentum vector. As seen from Fig. 6, an increasingly significant non-zero global polarization of Λ and anti-Λ is observed at STAR as the beam energy is scanned down [69]. The significance of the signal considering all energies is just over 7σ for Λ and 4.6σ for $\bar{\Lambda}$. It has been theorized [72, 73, 74] that this dependence may result from the depolarizing effect of higher temperatures at higher beam energies, or from a different rapidity distribution of the fireball's angular momentum as the beam energy changes.

As a result of this observation of global polarization, the rotational properties of the medium created in nuclear collisions are experimentally accessible for the first time. Vorticity, which can be defined in terms of the curl of the medium's velocity vectors in the non-relativistic limit, is proportional in a hydrodynamic picture to the summed polarization of both Λ and $\bar{\Lambda}$, with

appropriate corrections for Λ and $\bar{\Lambda}$ coming from the decay of heavier particles [69]. Given the fact that heavy-ion vortices are much smaller than those that arise in any other area of science, and of course are moving at relativistic speeds, it is not surprising that the the extracted energy-averaged vorticity, $\sim 9 \times 10^{21}$ s^{-1}, far exceeds any previous reported measurement (the closest is 10^7 s^{-1} for superfluid nanodroplets [75]). Models yield the right order of magnitude for the vorticity in nuclear collisions, but the calculated vorticity and its duration are subject to large uncertainties [76].

Particles with intrinsic magnetic moments interact with the intense magnetic field during a heavy-ion collision, and this is expected to result in a larger global polarization for $\bar{\Lambda}$ than for Λ [77]. In Fig. 6, a suggestion of such a difference is indeed observed, but averaged over all beam energies it is about a 2σ effect, and therefore STAR has deferred further probing of the heavy-ion magnetic field until the much larger statistics of BES-II become available.

8. Plans for Beam Energy Scan Phase-II

In order to revisit the several promising signals from BES-I analysis with greatly improved statistics, the follow-up BES-II program will take data in 2019 and 2020. The total beam time to be expended during BES-II will be comparable to that for BES-I, and the improved physics capability will come partly from three STAR detector upgrades, and partly from better RHIC luminosity.

The iTPC consists of new inner endcap sectors for the main STAR Time Projection Chamber. It replaces aged wires, and it changes the sparse pads of the old inner sectors to pads that cover the full area. This leads to better particle ID from dE/dx, and most important, it adds about 50% more pseudorapidity acceptance. A fourth iTPC benefit is extended acceptance at low transverse momentum, from $\sim$ 125 GeV/c to as low as 60 GeV/c. Another upgrade is the new Event Plane Detector (EPD). The EPD will have much improved event plane resolution compared with the Beam-Beam Counters currently used for that purpose, and will also be an excellent and flexible device for triggering and background rejection. The third upgrade is the endcap TOF detector (eTOF) on loan from the CBM collaboration at FAIR (Darmstadt). eTOF will improve particle ID in the new pseudorapidity acceptance region added by the iTPC.

The other main leg of the BES-II improvements comes from the RHIC machine. At $\sqrt{s_{NN}} \sim 12$ GeV and below, electron cooling will boost luminosity, while above that energy, there is a list of accelerator improvements involving bunch structure and β^*. The machine upgrades will deliver a nominal luminosity improvement over BES-I that ranges from a factor of $\sim$10 at 19.6 GeV to $\sim$25 at 7.7 GeV. Taking account of detector and RHIC upgrades, the STAR collaboration has documented many projected improvements in physics capabilities [78, 79].

RHIC luminosity in normal collider mode decreases like relativistic γ^3 at low energies, where the RHIC ring is used as a decelerator, and going below $\sqrt{s_{NN}} = 7.7$ GeV is not feasible in collider mode. However, allowing the halo of one of the RHIC beams to graze a fixed target inside the beam pipe at one end of the TPC leads to a reasonable acceptance over the forward half of rapidity space and allows enough events to be generated to easily saturate the DAQ bandwidth down to $\sqrt{s_{NN}} \sim 3$ GeV and below [80].

In a brief fixed-target test in 2015, it only required about a half hour of beam to acquire a million good Au + Au events with excellent trigger efficiency. This fixed target running therefore needs only a modest investment of beam time to extend μ_B coverage (at chemical freeze-out) from 420 MeV up to at least 720 MeV ($\sqrt{s_{NN}} = 3.0$ GeV or below), and in particular, to explore the crucial region where the net-proton kurtosis is predicted to drop back down to the baseline level (see Section 5).

9. Conclusions and outlook

BES-I at STAR has been very fruitful: final results are published in the case of 18 journal papers [21, 22, 23, 24, 25], with three further BES papers now in the refereeing process [19, 69, 81] and several more in earlier stages of the pipeline. These proceedings summarize two of the three BES-I goals, namely, the search for a 1st-order phase transition and critical point. Directed flow measurements point to a softest point in the QCD equation of state, but so far, overall model agreement with data is too poor for a clear conclusion about the nature of the phase transition. High-moment fluctuations and pion pair femtoscopy independently hint at a possible critical point; the former call for much better statistics and extended beam energy coverage on the low side, while conclusions from the latter require more study. There are excellent prospects for decisive progress in each of the above areas after the much enhanced data from BES-II in 2019 and 2020 become available.

These proceedings also touch on novel and exciting BES effects related to the heavy-ion magnetic field and vorticity, which were not even anticipated at the time when BES-II goals were formulated. With BES-II data, there are prospects for breakthrough-level progress in these topics, especially the first experimental determinations of the transient magnetic field in non-central heavy-ion collisions.

References

[1] Arsene I *et al.* (BRAHMS Collaboration) 2005 *Nucl. Phys.* A **757** 1
[2] Back B B *et al.* (PHOBOS Collaboration) 2005 *Nucl. Phys.* A **757** 28
[3] Adams J *et al.* (STAR Collaboration) 2005 *Nucl. Phys.* A **757** 102
[4] Adcox K *et al.* (PHENIX Collaboration) 2005 *Nucl. Phys.* A **757** 184
[5] Karsch F *et al.* 2004 *Nucl. Phys. Proc. Suppl.* **129** 614
[6] Aoki Y, Endrodi G, Fodor Z, Katz S D and Szabo K K 2006 *Nature* **443** 675
[7] Cheng M *et al.* 2009 *Phys. Rev.* D **79** 074505
[8] Fodor Z and Katz S D 2004 *J. High Energy Phys.* **04** 204
[9] Datta S, Gavai R V and Gupta S 2013 *PoS Lattice 2013* 202
[10] Kaczmarek O *et al.* 2011 *Phys. Rev.* D **83** 014504
[11] Bazavov A *et al.* 2012 *Phys. Rev.* D **85** 054503
[12] Ejiri S 2008 *Phys. Rev.* D **78** 074507
[13] Bowman E S and Kapusta J I 2009 *Phys. Rev.* C **79** 015202
[14] Rischke D H *et al.* 1995 *Heavy Ion Phys.* **1** 309
[15] Stöcker H 2005 *Nucl. Phys.* A **750** 121
[16] Stephanov M 2011 *J. Phys. G: Nucl. Part. Phys.* **38** 124147
[17] Ackermann K H *et al.* 2003 *Nucl. Instr. Meth.* A **499** 624
[18] Llope W for the STAR Collaboration 2012 *Nucl. Instr. Meth.* A **661** S110
[19] Adamczyk L *et al.* (STAR Collaboration) 2017 *Preprint* arXiv:1701.07065
[20] Cleymans J, Oeschler H, Redlich K and Wheaton S 2006 *Phys. Rev.* C **73** 034905
[21] Adamczyk L *et al.* (STAR collaboration) 2014 *Phys. Rev. Lett.* **112** 162301
[22] Adamczyk L *et al.* (STAR collaboration) 2014 *Phys. Rev. Lett.* **113** 052302
[23] Adamczyk L *et al.* (STAR collaboration) 2014 *Phys. Rev. Lett.* **113** 092301
[24] Adamczyk L *et al.* (STAR collaboration) 2015 *Phys. Rev.* C **92** 014904
[25] Adamczyk L *et al.* (STAR collaboration) 2016 *Phys. Rev.* C **94** 034908
Adamczyk L *et al.* 2016 *Phys. Rev. Lett.* **116** 112302
Adamczyk L *et al.* 2016 *Phys. Rev.* C **93** 014907
Adamczyk L *et al.* 2016 *Phys. Rev.* C **94** 024909
Adamczyk L *et al.* 2016 *Phys. Rev.* C **93** 021903
Adamczyk L *et al.* 2015 *Phys. Rev. Lett.* **114** 252302
Adamczyk L *et al.* 2015 *Phys. Lett.* B **750** 64
Adamczyk L *et al.* 2015 *Phys. Rev.* C **92** 021901
Adamczyk L *et al.* 2014 *Phys. Rev. Lett.* **112** 032302
Adamczyk L *et al.* 2013 *Phys. Rev.* C **88** 014902
Adamczyk L *et al.* 2013 *Phys. Rev. Lett.* **110** 142301
Adamczyk L *et al.* 2012 *Phys. Rev.* C **86** 054908
Agakishiev G *et al.* 2012 *Phys. Rev.* C **85** 014901

Abelev B I *et al.* 2010 *Phys. Rev.* C **81** 024911
[26] Konchakovski V P, Cassing W, Ivanov Y B and Toneev V D 2014 *Phys. Rev.* C **90** 014903
[27] Ivanov Yu B and Soldatov A A 2015 *Phys. Rev.* C **91** 024915
[28] Nara Y, Niemi H, Ohnishi A and Stöcker H 2016 *Phys. Rev.* C **94** 034906
[29] Singha S, Shanmuganathan P and Keane D 2016 *Adv. High Energy Phys.* **2016** 2836989
[30] Steinheimer J, Auvinen J, Petersen H, Bleicher M and Stöcker H 2014 *Phys. Rev.* C **89** 054913
[31] Nara Y, Niemi H, Steinheimer J and Stöcker H 2016 *Preprint* arXiv:1611.08023
[32] Voloshin S and Zhang Y 1996 *Z. Phys.* C **70** 665
[33] Poskanzer A M and Voloshin S A 1998 *Phys. Rev.* C **58** 1671
[34] Bilandzic A, Snellings R and Voloshin S 2011 *Phys. Rev.* C **83** 044913
[35] Bass S A *et al.* 1998 *Prog. Part. Nucl. Phys.* **41** 225
[36] Bleicher M *et al.* 1999 *J. Phys.* G **25** 1859
[37] Heinz U W 2010 *Relativistic Heavy Ion Physics* (Landolt-Boernstein New Series vol I/23) ed R Stock (New York: Springer Verlag)
[38] Sorge H 1997 *Phys. Rev. Lett.* **78** 2309
[39] Kolb P and Heinz U 2003 *Preprint* arXiv/nucl-th/0305084
[40] Huovinen P and Ruuskanen P V 2006 *Annu. Rev. Nucl. Part. Sci.* **56** 163
[41] Shanmuganathan P for the STAR Collaboration 2016 *Nucl. Phys.* A **956** 260
[42] Csernai L P and Stöcker H 2014 *J. Phys.* G **41** 124001
[43] Singha S for STAR Collaboration 2016 *Proc. Strangeness Quark Matter (Berkeley) Preprint* arXiv:1610.07423
[44] Kharzeev D 2006 *Phys. Lett.* B **633** 260
[45] Kharzeev D E, McLerran L D and Warringa H J 2008 *Nucl. Phys.* A **803** 227
[46] Buividovich P V, Chernodub M N, Luschevskaya E V and Polikarpov M I, 2009 *Phys. Rev.* D **80** 054503
[47] Bzdak A, Koch V and Liao J 2013 *Lect. Notes Phys.* **871** 503
[48] Kharzeev D E 2015 *Ann. Rev. Nucl. Part. Sci.* **65** 0000
[49] Miransky V A and Shovkovy I A 2015 *Phys. Rept.* **576** 1
[50] Huang X G 2016 *Rep. Prog. Phys.* **79** 076302
[51] D. Kharzeev D, Liao J, Voloshin S A and Wang G 2016 *Prog. Part. Nucl. Phys.* **88** 1 *Preprint* arXiv:1511.04050
[52] Abelev B I *et al.* (ALICE Collaboration) 2013 *Phys. Rev. Lett.* **110** 021301
[53] Deng W T, Huang X G, Ma G L and Wang G 2016 *Phys. Rev.* C **94** 041901
[54] Ling B and Stephanov M 2016 *Phys. Rev.* C **93** 034915
[55] Stephanov M A 2009 *Phys. Rev. Lett.* **102** 032301
[56] Asakawa M, Ejiri S and Kitazawa M 2009 *Phys. Rev. Lett.* **103** 262301
[57] Stephanov M A 2011 *Phys. Rev. Lett.* **107** 052301
[58] Gavai R V and Gupta S 2011 *Phys. Lett.* B **696** 459
[59] Adare A *et al.* (PHENIX Collaboration) 2016 *Phys. Rev.* C **93** 011901(R)
[60] Luo X, Mohanty B and Xu N 2014 *Nucl. Phys.* A **931** 808
[61] Luo X F and Xu N 2017 *Preprint* arXiv:1701.02105
[62] Lisa, M A, Pratt S, Soltz, R and Wiedemann U 2005 *Ann. Rev. Nucl. Part. Sci.* **55** 357
[63] Lacey R 2015 *Phys. Rev. Lett.* **114** 142301
[64] K. Aamodt *et al.* (ALICE Collaboration), *Phys. Lett.* B **696** 328
[65] Kleinert H 1999 *Phys. Rev.* D **60** 085001
[66] Andrea Pelissetto E V 2002 *Phys. Rept.* **368** 549 0012164.
[67] Ladrem M and Ait-El-Djoudi A 2005 *Eur. Phys. J.* C **44** 257
[68] Abelev B I *et al.* (STAR Collaboration) 2007 *Phys. Rev.* C **76** 024915
[69] Adamczyk L *et al.* (STAR Collaboration) 2017 *Preprint* arXiv:1701.06657
[70] Olive K A *et al.* 2014 *Chin. Phys.* C **38** 090001
[71] Bunce G *et al.* 1976 *Phys. Rev. Lett.* **36** 1113
[72] Betz B, Gyulassy M and Torrieri G 2007 *Phys. Rev.* C **76** 044901
[73] Jiang Y, Lin Z W and Liao J 2016 *Phys. Rev.* C **94** 044910
[74] Pang L G, Petersen H, Wang Q and Wang X N 2016 *Phys. Rev. Lett.* **117** 192301
[75] Gomez L F *et al.* 2014 *Science* **345** 906
[76] Becattini F *et al.* 2015 *Eur. Phys. J.* C **75** 406
[77] Becattini F, Karpenko I, Lisa M, Upsal I and Voloshin S 2016 *Preprint* arXiv:1610.02506
[78] STAR collaboration 2014 *STAR Note* 0598
[79] STAR Collaboration and CBM Collaboration eTOF Group 2016 *Preprint* arXiv:1609.05102
[80] Meehan K for the STAR Collaboration 2017 *Quark Matter presentation* https://indico.cern.ch/event/433345/contributions/2358275/
[81] Adamczyk L *et al.* (STAR Collaboration) 2017 *Preprint* arXiv:1701.06496